Dynamic Performance Improvement of DC Microgrids Using Virtual Impedance

Mehran Jami, Qobad Shafiee, Hassan Bevrani

Published (to be published) in: ***IEEE Xplore Digital Library***

(Expected) publication date: **2018**

Citation format for published version:
Mehran Jami, Qobad Shafiee, Hassan Bevrani. (2018). Dynamic Performance Improvement of DC Microgrids Using Virtual Impedance. *2018 Smart Grid Conference (SGC).* Univeristy of Kurdistan, Sanandaj, Kurdistan: IEEE Xplore Digital Library.

2018 Smart Grid Conference (SGC)

Dynamic Performance Improvement of DC Microgrids Using Virtual Impedance

Mehran Jami, Qobad Shafiee, *Senior Member, IEEE*, Hassan Bevrani, *Senior Member, IEEE*
Smart/Micro Grids Research Center (SMGRC)
Department of Electrical Engineering University of Kurdistan
Sanandaj, Iran
m.jami@eng.uok.ac.ir, q.shafiee@uok.ac.ir, bevrani@uok.ac.ir

***Abstract*—In DC microgrids, classical generators in traditional power grid are replaced by converter-interfaced distributed generation (DG) or energy storage systems (ESSs) and rotating inertia cannot be directly connected. This causes a reduction of the total inertia of the system. Therefore, the DC microgrid voltage becomes more sensitive under load variations and power fluctuation from the intermittent distributed energy sources. In this paper a virtual-impedance control is designed for DC microgrids, which provides the system with synthetic inertia. In proposed strategy, the rate of change of voltage (RoCoV) can be decreased by virtual-capacitor part, transient and steady-state behavior of the converter under load variations can be defined by varying the virtual-inductance and virtual-resistance, respectively. Stability of the proposed strategy is analyzed by looking at the dominant eigenvalues of the small-signal model. The simulation results indicate that the proposed method with virtual impedance improves the transient response.**

Keywords—DC Microgrid, dynamic response, virtual impedance, virtual capacitance, virtual inductance.

I. INTRODUCTION

Distributed generation (DG) approach has been widely accepted in recent years due to the concerns about the energy, global warming, climate changes and reduction of the fossil fuels. Since the existing power systems are based on AC systems, the recent literature on the MGs has mostly focused on AC MGs. In recent years, the research attention on DC grids has been resurged due to technological advancements in power electronics and energy storage devices [1]. From the generating side, renewable energy resources such as photovoltaic (PV), fuel cell and wind systems are inherently DC or converted to DC. Moreover, common energy storage (ES) units (e.g., batteries and ultra-capacitors) use DC voltage. From the load side, electronic loads such as computers and data centers, motor drives, LED lighting, electric vehicle chargers require a DC supply. Several advantages of DC-MGs compared to AC-MGs, including easier control schemes due to the lack of frequency and reactive power control, can overcome inrush currents, frequency synchronization and harmonics. In addition, it improves overall efficiency, power quality, reliability, and lower costs [2]. Against all the advantages of DC-MGs, their voltage regulation is a challenging task due to their poor nature under deviation, frequent load steps and intermittent generations. This is even more considerable in the islanded operation because, unlike conventional bulk power plants, at MG, instantaneous power changes are not performed by rotary generators with high inertia directly connected to the grid. Instead, these generators are replaced by converter-interfaced generation or storage systems that essentially do not provide any transient responses to power changes [3]. Limited generational inertia and damping elements cause stability concerns when supplying light loads. Therefore, virtual inertia is a promising and effective way to solve the problem without introducing additional cost or loss [4]. Thus, researching on this topic has great significance. Since the last years, many studies have been done on the virtual inertia control, focusing on the AC-MG. One of these approaches is the imitating the behavior of synchronous generators. These techniques are known as virtual synchronous machines (VSM) [5]. This concept is rarely used for DC-MG. By imitation of VSM, a virtual inertia control strategy is proposed to enhance the inertia of the DC-MG [4], [6], [7]. Increasing the inertia of photovoltaic (PV) system through inertia emulation is proposed in [8] and an adaptive virtual inertia control strategy with the variable droop coefficient is suggested to increase the inertia of the DC-MG in [9].

Virtual impedance loops are added to the control systems of converter for soft-starting of voltage source inverters, increasing the accuracy of real power sharing [10], compensating voltage imbalance in islanded DC-MG [11]. In order to avoid adding physical capacitors to the bus of the MG, some authors have proposed virtual-capacitance-based control techniques which provide synthetic capacitance to the system [12]. This method is not useful against load changes. Therefore, the virtual impedance loop is equipped with inductive impedance to improve the dynamic performance of the power sharing control unit [13]. An admittance type droop control with additional capability of introducing virtual inertia to the system is proposed in [14].

In this paper, an impedance-type RC-L-mode droop control method is proposed to introduce virtual inertia into DC MG. In [12] virtual impedance includes only capacitance and resistance. Also implementation of this method does not improve voltage response with load changes and power input voltage change. In [14], authors remove voltage and droop controller and do not consider virtual inductance. The proposed control structure improves dynamic performance with load variation, change reference voltage and output voltage of distributed generations.

978-1-7281-1138-4/18/$31.00©2018 IEEE

Capacitance and inductance terms of impedance improve response of system to change voltage reference and load variations, respectively.

The rest of this paper is outlined as follows: Section II introduce the virtual impedance control strategy. In Section III, the small-signal model is derived and validated via time-domain simulation for operation point variations. Stability analysis and range of parameters are discussed in Section IV. Simulations results are presented in Section V. Finally, conclusions are provided in Section VI.

II. VIRTUAL IMPEDANCE CONTROL STRATEGY FOR DC-MGS

Fig. 1 illustrates the structure of the proposed virtual impedance control strategy employed by the buck converter. As it can be observed, the inner loop control is composed by classical cascaded current and voltage proportional-integral (PI) regulators. At higher level, a virtual impedance loop assigned the output voltage reference. In case of DC MGs, the most frequently used droop method is the V-I droop (virtual resistance) control, can be merged with the virtual impedance loop. The main parts of the virtual impedance include the virtual inductor and the virtual capacitor.

For the AC-MGs, inertia of the system shows the ability to avoid sudden changes of the frequency, by releasing its stored energy, and thereby synchronous machine (SM) will have enough time to regulate the active power *P*o. The power balance equation can be described as [4]

$$P_{set} - P_o - D_p\left(\omega - \omega_n\right) = J\omega\frac{d\omega}{dt} \approx J\omega_n\frac{d\omega}{dt} \tag{1}$$

Where Pset, Po, Dp, ω, and ωn are the active power reference, the output power, the damping coefficient, the angular frequency, and the rated angular frequency of the utility grid, respectively. J is the virtual moment of inertia. For the DC-MG, inertia of the system shows the ability to avoid sudden changes of the dc bus voltage u. The kinetic energy Wr saved in the rotor of the synchronous machine, and the electric energy Wc saved in the capacitors connected to the dc bus in DC-MG and magnetic energy Wl saved in the inductive are defined as

$$W_r = \frac{1}{2}J\omega^2 \quad , \quad W_c = \frac{1}{2}Cu^2 \quad , \quad W_l = \frac{1}{2}Li^2 \tag{2}$$

In the DC-MG, the virtual inertia strategy becomes a virtual capacitor and virtual inductance concept. According to the mentioned analysis, it is apparent that there is a dual relationship between variables in equation (1) containing SM and DC-MG containing virtual capacitance (VC) and virtual inductance (VI), as shown in Table I. Thus the current balancing equation can be described as

$$i_{set} - i_o = \frac{1}{R_v}\left(u - U_n\right) + C_V\frac{d\left(u - U_n\right)}{dt} = -i_v \tag{3}$$

Where i_{set}, i_o, u, U_n, R_V, C_V and i_v are the dc output current reference, the dc output current, the DC bus voltage, the rated DC bus voltage, the virtual resistance, virtual capacitance and the desired current injection of virtual

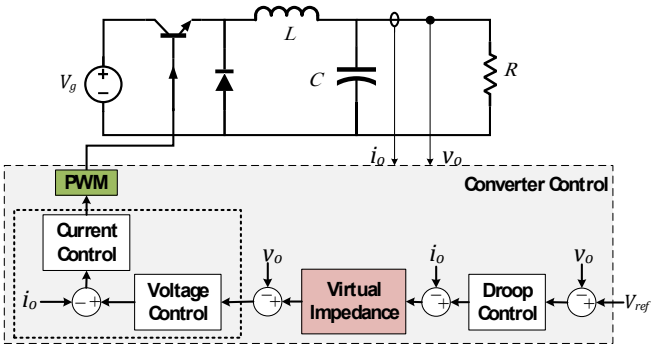

Fig. 1. Proposed virtual-impedance control strategy for buck converter.

TABLE I. ANALOGY BETWEEN AC-MG AND DC-MG

Microgrids	AC-MG containing VSM	DC-MG containing VC	DC-MG containing VI
Control goal	ω	u	i
Output	P_o	i_o	v_o
Damping	D_p	$1/R_V$	R'_V
Inertia	$J\omega_n$	C_V	L_V

inertia control, respectively. The transfer function between $\Delta u(s)$ and $i_v(s)$ is as follows

$$-\frac{\Delta u(s)}{i_v(s)} = \frac{1}{C_V s + 1/R_V} \tag{4}$$

Therefore, the modified droop control function become

$$u = U_n - i_v(s)\left(\frac{1}{C_V s} \,||\, R_V\right) \tag{5}$$

This impedance includes parallel capacitance and resistance. This structure is not useful against load changes. Therefore, the virtual impedance loop is equipped with inductive impedance to improve the dynamic performance of the power sharing control unit. This control structure improves dynamic performance with load variation, change voltage reference and output voltage of distributed generations. According to the mentioned analysis, it is apparent that there is a dual relationship between the virtual inertia against voltage variation that modeled with virtual capacitance and the virtual inertia against current variation that modeled with virtual inductance. Thus the voltage balancing equation can be described as

$$v_{set} - v_o = R'_V\left(i - I_n\right) + L_V\frac{d\left(i - I_n\right)}{dt} = -v_v \tag{6}$$

Where v_{set}, v_o, i, I_n, R'_V, L_V and v_v are the dc output voltage reference, the dc output voltage, the DC bus current, the rated DC bus current, the virtual resistance, virtual inductance and the desired voltage of virtual inertia control, respectively. The transfer function between $\Delta i(s)$ and $v_v(s)$ as follows

$$-\frac{\Delta i(s)}{v_v(s)} = \frac{1}{L_V s + R'_V} \tag{7}$$

Therefore, the modified droop control function become

$$i = I_n - \frac{v_v(s)}{(R_V' + L_V s)} \tag{8}$$

This impedance includes series inductance and resistance. Fig. 2 shows combined virtual inertia against voltage variation that modeled with virtual capacitance and the virtual inertia against current variation that modeled with virtual inductance.

III. Small-Signal Modeling

In order to find out the relation between the dc bus voltage, power demand, voltage reference and output voltage of distributed generations of the DC-MG, it is necessary to build the buck converter small-signal model. In addition, the parametric stability analysis in this paper is based on the value of the dominant poles or eigenvalues of the full configuration of the proposed control strategy.

In [15], small-signal ac transfer function of a switching converter is obtained. Fig. 3 shows the equivalent circuit model of the buck converter. This model contains three independent inputs: the power input voltage deviations $\hat{v}_g$, the control input variation $\hat{d}$ and load current disturbance i_{load}. Each of these inputs effects on the output voltage and the output voltage variation $\hat{v}$ can be represented as a combination of the three input, as follows

$$\hat{v}(s) = G_{vd}(s)\hat{d}(s) + G_{vg}(s)\hat{v}_g(s) - Z_{out}(s)i_{load}(s) \tag{9}$$

Where G_{vd}, G_{vg} and Z_{out} are converter control to output transfer function, converter line to output transfer function and converter output impedance, respectively as follow

$$G_{vd}(s) = \left.\frac{\hat{v}(s)}{\hat{d}(s)}\right|_{\substack{\hat{v}_g(s)=0 \\ i_{load}(s)=0}} = \frac{V_g \omega_r^2}{s^2 + 2\xi s + \omega_r^2} \tag{10}$$

$$G_{vg}(s) = \left.\frac{\hat{v}(s)}{\hat{v}_g(s)}\right|_{\substack{\hat{d}(s)=0 \\ i_{load}(s)=0}} = \frac{D\omega_r^2}{s^2 + 2\xi s + \omega_r^2} \tag{11}$$

$$Z_{out}(s) = -\left.\frac{\hat{v}(s)}{i_{load}(s)}\right|_{\substack{\hat{v}_g(s)=0 \\ \hat{d}(s)=0}} = \frac{Ls\omega_r^2}{s^2 + 2\xi s + \omega_r^2} \tag{12}$$

Where V_g and D are steady-state value of power input voltage and duty cycle, respectively. the following parameters are defined

$$\omega_r = \frac{1}{\sqrt{LC}}, \qquad \xi = \frac{1}{RC} \tag{13}$$

A block diagram of a feedback system is shown in Fig. 4. Transfer function between output voltage variations and reference input voltage variations is

$$T_1(s) = \frac{\hat{v}(s)}{\hat{v}_{ref}(s)} = \frac{G_V(s)G_I(s)H(s)G_{vd}(s)/R_D}{1+T(s)} \tag{14}$$

The value of C_v and L_v only effect on transient response and not influence on steady-state response. The steady-state value depends on the droop resistance (R_D), virtual damping ($1/R_v$) and (R'_V) and load (R) that is obtained as follows

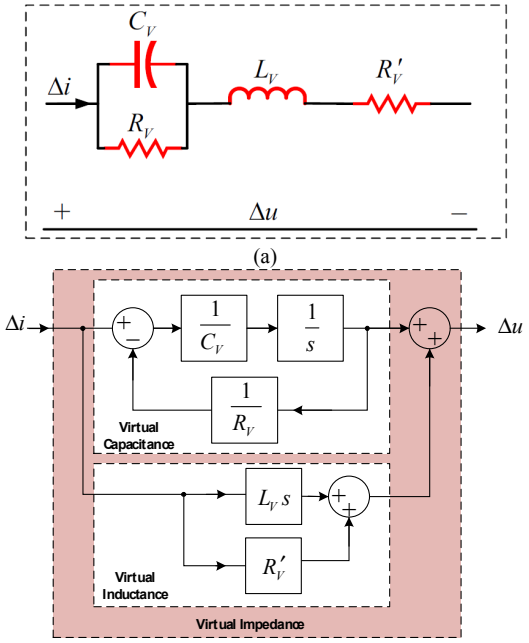

Fig. 2. Illustration of different part of virtual-impedance. (a) equivalent circuit of impedance-type droop method. (b) block diagram virtual impedance.

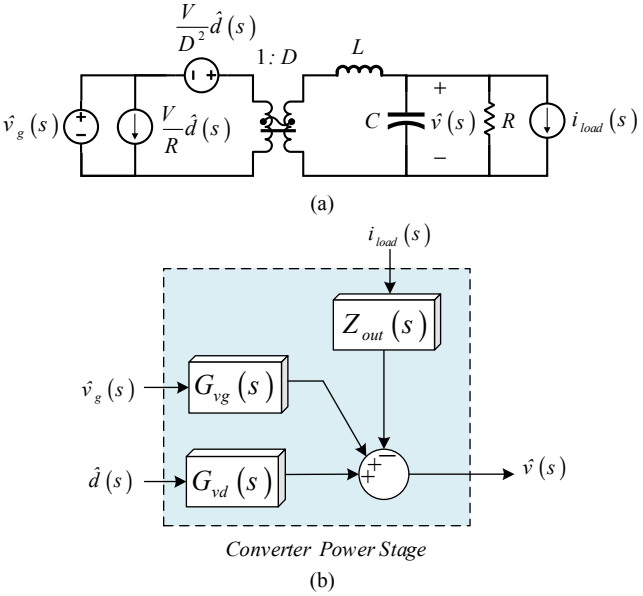

Fig. 3. Buck converter small-signal model which represents variation in v_g, d and i_{load}. (a) with converter equivalent circuit. (b) block diagram [15]

$$v_{ss} = \frac{V_{ref}}{1 + R_D/R + R_D/(R_V + R_V')} \tag{15}$$

R_D, R_v and R'_V adjustment DC bus voltage and improvement power sharing in DC-MG.

Transfer function between output voltage variations and power input voltage variations is

$$T_2(s) = \frac{\hat{v}(s)}{\hat{v}_g(s)} = \frac{G_{vg}(s)}{1+T(s)} \tag{16}$$

Transfer function between output voltage variations and load current variations is

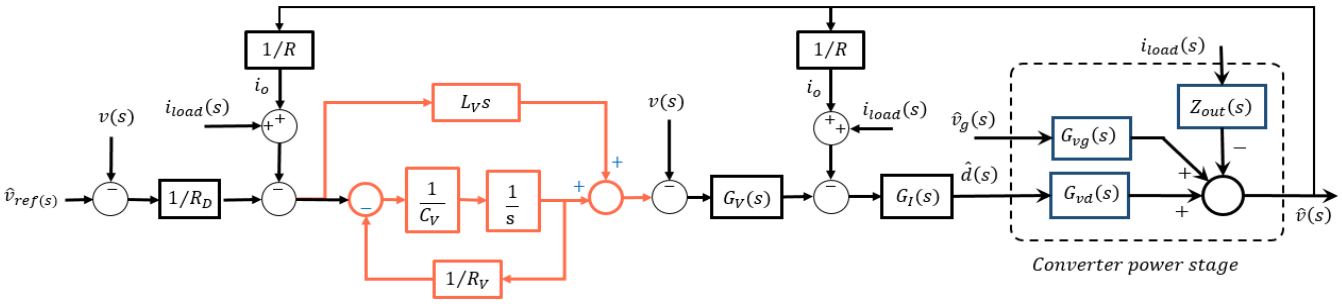

Fig. 4. Small-signal model of the virtual impedance control system.

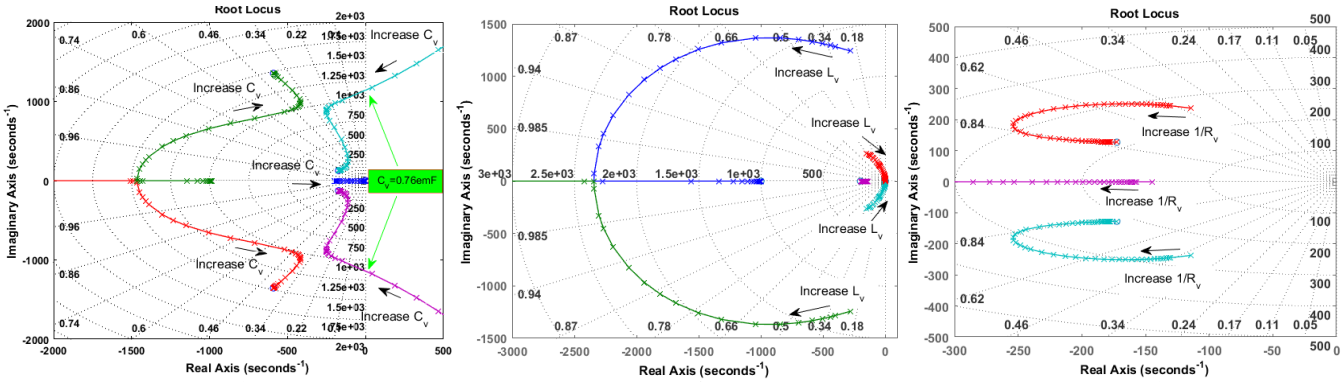

(a) (b) (c)

Fig. 5. Trace of the system eigenvalues. (a) varying C_v for L_v=0.5 mH and R_v=100 Ω. (b) varying L_v for C_v=0.01 F and R_v=100 Ω. (c) varying R_v for L_v=0.5 mH and C_v=0.01 F

$$T_3(s)=\frac{\hat{v}(s)}{i_{load}(s)}= \frac{-Z_{out}(s)-G_V(s)G_I(s)H(s)G_{vd}(s)-G_I(s)G_{vd}(s)}{1+T(s)} \tag{17}$$

That in the above equations *H(s)* is the transfer function of virtual impedance loop. The loop gain *T(s)* is defined in general as the product of the gains around the feedback path of the loop. As follows

$$T(s)= G_{vd}(s)G_I(s)\left[G_V(s)H(s)\left(\frac{1}{R_D}+\frac{1}{R}\right)+G_V(s)+\frac{1}{R}\right] \tag{18}$$

and

$$H(s)=\frac{1}{C_V s+1/R_V}+L_V s+R_V' \tag{19}$$

Solution of Fig. 4 for the output voltage variation *v* yields

$$\hat{v}(s)=T_1(s)\hat{v}_{ref}(s)+T_2(s)\hat{v}_g(s)+T_3(s)i_{load}(s) \tag{20}$$

IV. System Stability Analysis

One of the main challenges for the design of control strategies is to define the parameters of regulators so that the system operates adequately at different operation points. Moreover, it is important to identify how these parameters as well as other variables will affect the behavior and response of the system. The stability analysis is a useful tool in order to define these values and design control strategies that ensure a stable operation for all the working range [16].

This section focuses on the stability analysis and damping performance improvement of buck converter in DC-MG. The small-signal model of a virtual impedance control system has been derived. Eigenvalue analysis results determine the relationship between the system stability and different factors of control method, including the virtual capacitance, virtual inductance and virtual damping that modeled with virtual resistance. For each input, characteristic equation of the system is same and the poles of the system are its roots that is obtained as follows

$$1+T(s)=0 \tag{21}$$

Fig. 5(a) shows the dominant poles distribution diagram of the system with C_v changing. For L_v=0.5 mH, R_v=100 Ω and virtual capacitor values less than C_v=0.76 mF two poles will move to the right half plane so that the system is unstable. Therefore, for the stability of system, it is satisfactory enough when C_v > 0.76 mF. by increasing C_v, damping factor increase and the overshoot of the system and frequency of oscillations decrease. When C_v increasing, inertia of the DC-MG becomes larger, and the operation of the dynamic response slows down, which reduce the impact of the dc bus voltage caused by power fluctuation of the DC-MG. vice versa, when C_v is smaller, inertia of DC-MG becomes smaller and its ability to suppress the dc bus voltage fluctuation weakens.

Fig. 5(b) shows the eigenvalues distribution and trajectory of the system with L_v changing. For any virtual inductance values the system is stable. Though, by increasing L_v, dominant poles will move to the right side of plane so that the system damping factor and frequency of oscillations decrease and the overshoot of the system increase.

Fig. 5(c) shows the dominant poles distribution diagram of the system with R_v changing. For any virtual resistance values the system is stable. Though, by decreasing R_v, 1/ R_v increases dominant poles will move to the left side of plane so that the system damping factor and the overshoot of the system decrease.

V. Simulation Results and Verification

In order to demonstrate the effectiveness of the proposed control strategy, the buck converter system of Fig. 1 is simulated. The model of Fig. 1 is implemented base on MATLAB/Simulink and the parameters are given in Table II. The small-signal transfer function model is linearized over a point of operation determined by the values shown in Table II. At the instant t = 0.2 s, the reference voltage is varied a 20% from V_{ref} =50 V to V_{ref} =60 V and power input voltage is varied a 20% from V_g =100 V to V_g =120 V and load current is varied a 20% from i_{load} =4.7 A to i_{load} =5.6 A. Fig. 6 shows the response of the nonlinear and small-signal transfer function linearized model under this current variation. The results show a good accuracy of the linearized model even for a 20% variation over the linearization point, which validates the model for the following stability analysis. Fig. 7 shows the DC bus voltage under virtual capacitance variation and virtual inductance constant. Fig. 7(a) illustrates the DC bus voltage with the reference voltage is varied a 20% from V_{ref} =50 V to V_{ref} = 60 V at the instant t = 0.2 s and return to primary state at t =0.4 s. According to Fig. 5(a), for the stability of system, it is satisfactory enough when C_v > 0.76mF. When C_v increasing, inertia of the DC-MG becomes larger, and the operation of the dynamic response slows down and makes it avoid of sudden voltage changes. This feature provides enough time for reaction to variation. Fig. 7(b) illustrates the DC bus voltage with the power input voltage is varied a 20% from V_g = 100 V to V_g = 120 V at the instant t = 0.2 s. When C_v increasing, voltage fluctuation and undershoot of voltage decrease and improves dynamic response of the system. However, voltage fluctuation is not completely damped and overshoot has not changed. By increasing the virtual capacitance from the certain value, change in response will not be made. Fig. 7(c) illustrates the DC bus voltage with the load current is varied a 20% from i_{load} = 4.7 A to i_{load}=5.6A at the instant t = 0.2 s. When C_v increasing, voltage fluctuation and overshoot of voltage decrease and improves dynamic response of the system. However, voltage fluctuation is not completely damped and undershoot has not changed. By increasing the virtual capacitance from the certain value, change in response will not be made. Fig. 8 shows the DC bus voltage under virtual inductance variation and virtual capacitance constant. Fig. 8(a) illustrates the DC bus voltage with the reference voltage is varied a 20% from V_{ref} = 50 V to V_{ref} = 60 V at the instant t=0.2s. When L_v increasing, siting time and overshoot increase. DC bus voltage oscillation with the reference voltage varying is a one of the weaknesses proposed control strategy. However, this behavior similar to inertia and the operation of the dynamic response slows down. As the virtual inductance increases, these fluctuations increases. as a result, for better dynamic performance in reference voltage change, increase C_v favorable than increase L_v. Fig. 8(b) shows the simulation waveforms of the dc bus voltage when the power input voltage of the buck converter V_g suddenly changes. When t = 0.2 s, V_g suddenly increase from 100 to 120 V. When L_v increasing, voltage fluctuation, undershoot and overshoot of voltage decrease and improves dynamic response of the system better than Fig. 7(b). as a result, for better dynamic performance in power input voltage change, increase L_v favorable than increase C_v. Fig. 8(c) shows the simulation waveforms of the dc bus voltage when the load current of the buck converter i_{load} suddenly changes. When t = 0.2 s, i_{load} suddenly increase from 4.7 to 5.6A. When L_v increasing, voltage fluctuation, undershoot and overshoot of voltage decrease and improves dynamic response of the system better than Fig. 7(c). as a result, for better dynamic performance in load current change, increase L_v favorable than increase C_v. The value of C_v and L_v only effect on transient response and not influence on steady-state response. The steady-state value depends on the droop resistance (R_D), virtual damping ($1/R_v$) and R'_v and load (R) that is obtained in (15).

TABLE II. System Parameters of the Virtual Impedance Control Method

Parameters	Values	Parameters	Values
L (mH)	10	k_{pv}	0.1
C (mF)	0.1	k_{iv}	100
R (Ω)	10	k_{pi}	0.05
V_g (V)	100	k_{ii}	10
f_s (KHz)	15	R_D (Ω)	0.5
V_{ref} (V)	50	R_v , R'_v (Ω)	100, 0
L_v (mF)	0.5	C_v (mF)	10

VI. Conclusion

Low inertia and dc bus voltage fluctuation imperil the secure and steady operation of the DC-MGs and reduce the system performance. In order to solve this problem, this paper presents a new control strategy for buck converter to improve the dynamic response of a DC-MGs. a virtual impedance control strategy for DC-MGs by analogy with the VSM in AC-MGs was proposed to enhance the inertia of the DC-MGs and to restrain the dc bus voltage fluctuation. One of the main advantages of this type of control in comparison with classical approaches is that the rate of change of the MG voltage can be decrease by simply varying the virtual capacitance. As a result, for better dynamic performance in reference voltage change, increasing C_v, for power input voltage change, increasing L_v and for load current change, increasing L_v. The small-signal model of the buck converter control system was built and the dynamic transfer function between the dc output voltage of the converter and the inputs was represented. Through eigenvalues analysis, the relationship between system stability and different factors in the control system is studied.

References

[1] H. Bevrani, B. Francois, and T. Ise, *Microgrid Dynamics and Control*, NJ, USA: Wiley, July 2017.

[2] T. Dragičević, X. Lu, J.C. Vasquez, and J.M. Guerrero, "DC microgrids—Part I: A review of control strategies and stabilization techniques," *IEEE Trans. Power Electron*., vol. 31, no. 7, pp. 4876-4891, Jul. 2016.

[3] H. Bevrani, T. Ise, and Y. Miura, "Virtual synchronous generators: A survey and new perspectives," *International Journal of Electrical Power & Energy Systems*, vol. 54, pp. 244-254, Jan. 2014.

[4] W. Wu, Y. Chen, A. Luo, L. Zhou, X. Zhou, L. Yang, Y. Dong, and J.M. Guerrero, "A virtual inertia control strategy for DC microgrids analogized with virtual synchronous machines, " *IEEE Trans. Ind. Electron.*, vol. 64, no. 7, pp. 6005-6016, Jul. 2017.

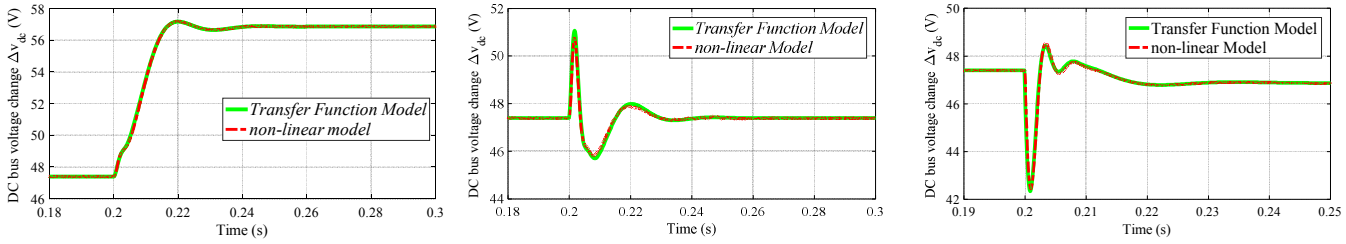

Fig. 6. Comparison of bus voltage response in the nonlinear and linearized model under 20% variation. (a) V_{ref} variation. (b) V_g variation. (c) i_{load} variation.

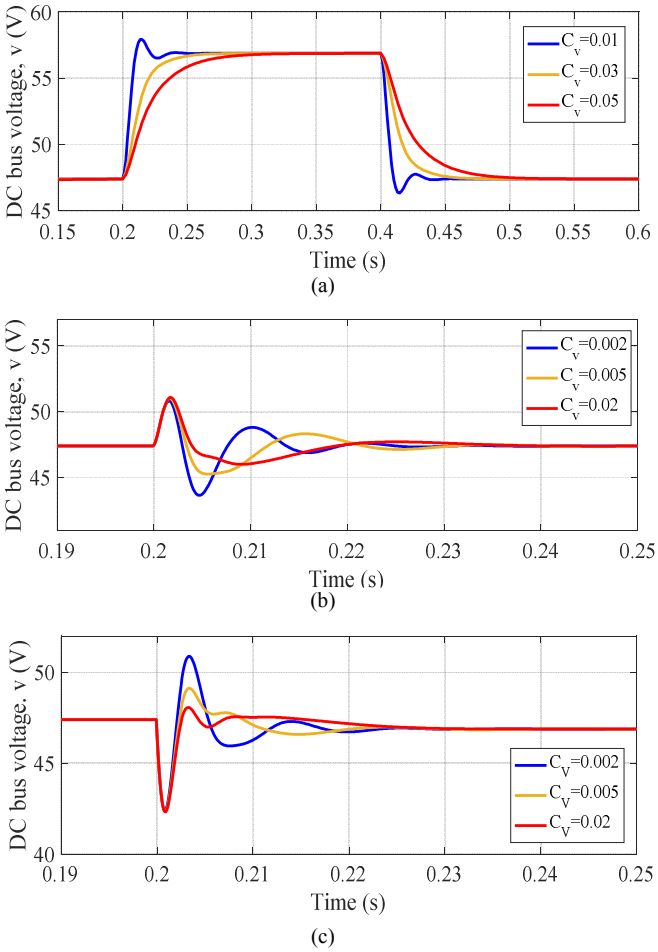

Fig. 7. DC bus voltage by varying C_v and L_v=0.5 mH. (a) The reference voltage increases a 0.2pu at t=0.2s and decrease 0.2pu at t=0.4s. (b) The power input voltage increases a 0.2pu at t=0.2s. (c) Load current increases a 0.2pu at t=0.2s.

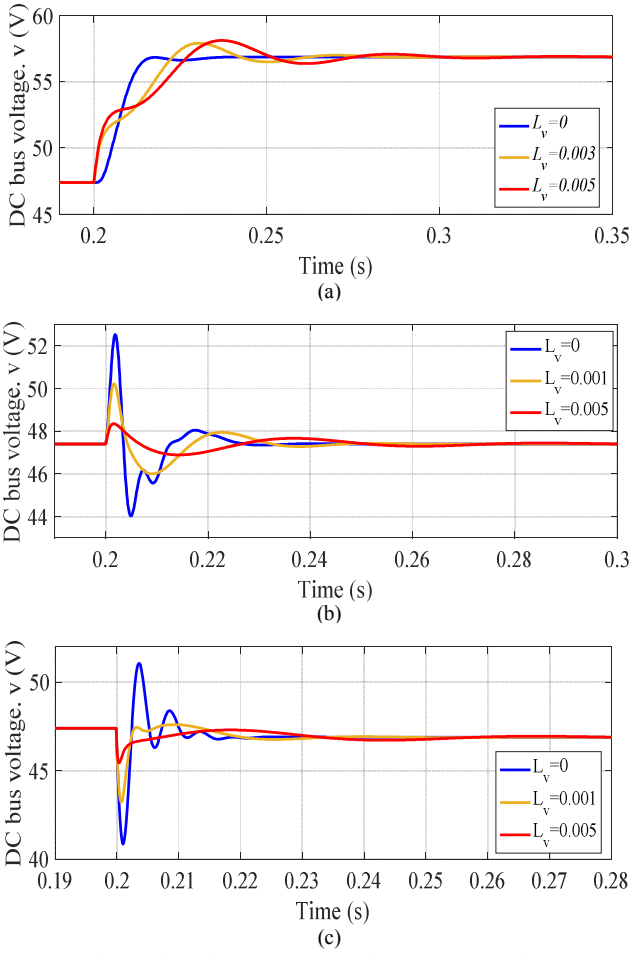

Fig. 8. DC bus voltage by varying L_v and C_v=0.01F. (a) The reference voltage increases a 0.2pu at t=0.2s. (b) The power input voltage increases a 0.2pu at t=0.2s. (c) Load current increases a 0.2pu at t=0.2s.

[5] D. Chen, Y. Xu, and A. Q. Huang, "Integration of DC Microgrids as Virtual Synchronous Machines into the AC Grid," *IEEE Trans. Ind. Electron.*, vol. 64, no. 9, pp. 7455–7466, Sep. 2017.

[6] Y. Li, L. He, F. Liu, C. Li, Y. Cao, and M. Shahidehpour, "Flexible voltage control strategy considering distributed energy storages for dc distribution network," *IEEE Trans. Smart Grid*, Jul. 2017.

[7] E. Rakhshani, and P. Rodriguez, "Inertia emulation in AC/DC interconnected power systems using derivative technique considering frequency measurement effects," *IEEE Trans. Power Syst.*, vol. 32, no. 5, pp. 3338-3351, Sep. 2017.

[8] W.S. Im, C. Wang, W. Liu, L. Liu, and J.M. Kim, "Distributed virtual inertia based control of multiple photovoltaic systems in autonomous microgrid," *IEEE/CAA Journal of Automatica Sinica*, vol. 4, no. 3, pp. 512-519, Nov. 2016.

[9] C. Wang, J. Meng, Y. Wang, and H. Wang, "Adaptive virtual inertia control for DC microgrid with variable droop coefficient," In *Electrical Machines and Systems (ICEMS), 2017 20th International Conference on* (pp. 1-5). IEEE, Oct. 2017.

[10] S. Agarwal, S. Islam, and S. Anand, "Dynamic droop gain adjustment for proportional power sharing in low voltage DC microgrid," In *Power Electronics, Drives and Energy Systems (PEDES), 2016 IEEE International Conference on* (pp. 1-6), Dec. 2016.

[11] M. Hamzeh, M. Ghafouri, H. Karimi, K. Sheshyekani, and J.M. Guerrero, "Power oscillations damping in DC microgrids," *IEEE Trans. Energy Convers.*, vol. 31, no. 3, pp. 970-980, Sep. 2016.

[12] E. Unamuno, J.A. and Barrena, "Design and small-signal stability analysis of a virtual-capacitor control for DC microgrids," In *Power Electronics and Applications (EPE'17 ECCE Europe), 2017 19th European Conference on* (pp. P-1), Sep. 2017.

[13] M. Hamzeh, M. Ashourloo, and K. Sheshyekani, "Dynamic performance improvement of DC microgrids using virtual inductive impedance loop," In *Power Electronics, Drive Systems and Technologies Conference (PEDSTC), 2014 5th* (pp. 452-457), Feb. 2014.

[14] Z. Jin, L. Meng, R. Han, J.M. Guerrero, and J.C. Vasquez, "Admittance-type RC-mode droop control to introduce virtual inertia in DC microgrids," In *Energy Conversion Congress and Exposition (ECCE), 2017 IEEE* (pp. 4107-4112), Oct. 2017.

[15] R. W. Erickson, and D. Maksimovic, *Fundamentals of power electronics.* Springer Science & Business Media, 2007.

[16] L. Guo, S. Zhang, X. Li, Y.W. Li, C. Wang, and Y. Feng, "Stability analysis and damping enhancement based on frequency-dependent virtual impedance for dc microgrids," *IEEE Journal of Emerging and Selected Topics in Power Electronics*, vol. *5*, no. 1, pp. 338-350, Mar. 2017.